Available online at www.sciencedirect.com
ScienceDirect
Sensors and Actuators A 142 (2008) 12–18
SENSORS AND ACTUATORS A PHYSICAL
www.elsevier.com/locate/sna

Optical characterization of silicon rich oxide films

A. Morales-Sánchez [a,*], J. Barreto [a], C. Domínguez-Horna [a], M. Aceves-Mijares [b], J.A. Luna-López [b]

[a] *IMB–CNM (CSIC), Campus UAB. 08193, Bellaterra, Barcelona, España*
[b] *INAOE, Electronics Department, Puebla, Pue., ZP 72000, México*

Received 30 September 2006; received in revised form 14 February 2007; accepted 10 March 2007
Available online 14 March 2007

Abstract

Silicon rich oxide (SRO) films with different silicon excess were deposited by low pressure chemical vapor deposition (LPCVD) using SiH_4 and N_2O as the reactant gasses. A set of SRO films was implanted with silicon ions (SI-SRO). After thermal annealing, SRO and SI-SRO films with low Si excess showed a strong visible photoluminescence (PL) in the 1.4–2.1 eV range, characteristic of silicon nanocrystals (Si-nc's) formation. For SRO layers, a redshift of the PL peak was only observed by increasing the silicon excess from 4 to 5.1 at. %, no redshift took place when the silicon excess was 12.7 at. %. The SI-SRO films exhibited a similar behaviour. For implanted and non implanted samples, transmission electron microscopy analysis only showed silicon clusters when the silicon excess was higher than 5 at. %. It has been observed that the Si-clusters size was larger as the silicon excess increased and that the Si-clusters density increased when the SRO films were implanted. Therefore, a stronger PL response was observed in the SI-SRO films. The structural and optical properties of SRO and SI-SRO films have been related, suggesting that the emission could be associated to Si-clusters/defects interaction.

PACS: 78.55.-m; 82.80.Gk; 82.80.Ej; 61.72.Tt

Keywords: Silicon rich oxide; Silicon clusters; Photoluminescence; FTIR; XPS; EFTEM

1. Introduction

Discovery of visible room temperature luminescence in porous silicon [1] attracted a new effective way to obtain light emission in silicon based materials. However, the porous silicon suffers from poor mechanical and chemical stability. Therefore, a great number of investigations have been carried out to find stable materials from the last decade. The silicon nanocrystals (Si-nc's) embedded in a SiO_2 matrix have attracted the main attention. One of the most studied materials has been the Silicon Rich Oxide (SRO), because the silicon excess separates from the oxide matrix and forms nanometer silicon grains dispersed throughout the oxide when the film is subjected to high temperature anneal. These materials have shown interesting properties in charge trapping [2] and electroluminescence [3,4], besides, they have been used with a PN junction to get a radiation sensor [5]. Different preparation techniques of SRO films have been reported, such as ion implantation of Si into thermal silicon oxide [4,6], Pulsed Laser Deposition (PLD) [7], Plasma Enhanced Chemical Vapor Deposition [7–11], thermal evaporation [12,13], as well as SiO/SiO_2 multilayers [3]. In spite of a great number of studies, the mechanism of light emission is still controversial; some authors have related the PL to Quantum Confinement Effects (QCE) in Si-nc's [11], and some other to defects [6] and localized states on the surface of Si-nc's and Si-clusters [14].

In this work, a study about composition, structure and optical properties of SRO and SI-SRO films obtained by LPVCD in order to obtain information that help to understand the mechanism of emission is reported. The effect of the silicon excess and silicon implantation on the PL response has been also studied.

2. Experiment

SRO films were deposited on n type (100) Si wafers in a LPCVD hot wall reactor using N_2O and SiH_4 as the reactant

* Corresponding author. Tel.: +34 93 594 77 00; fax: +34 93 580 14 96.
E-mail address: alfredo.morales@cnm.es (A. Morales-Sánchez).

0924-4247/$ – see front matter © 2007 Elsevier B.V. All rights reserved.
doi:10.1016/j.sna.2007.03.008

Table 1
Thickness and refractive index of SRO as deposited films

Ro=N_2O/SiH_4	Thickness (nm)	Refractive index as deposited
10	770	1.99
20	730	1.64
30	720	1.48

gasses at 700 °C. The flow ratio (Ro) between N_2O and SiH_4 was used to control the amount of silicon excess into the SRO films. The expected thickness of the films was around 700 nm. After deposition, Si ions were implanted into a set of SRO samples at energy of 150 keV and a dose of 5×10^{15} /cm^2. A Gaertner L117 ellipsometer was used to obtain the thickness and the refractive index of the films. After deposition and implantation, SRO and SI-SRO films were thermally annealed at 1100 °C for 60 minutes in N_2 atmosphere. Fourier transform infra-red spectroscopy was used to study the structure and composition of the films. The silicon excess in SRO and SI-SRO films was measured with a PHI ESCA – 5500 X–ray photoelectron spectrometer (XPS). Energy Filtered Transmission Electron Microscopy (EFTEM) images were obtained using an electronic microscopy JEOL JEM 2010F, all the EFTEM images were measured using a Si plasmon of 17 eV and cross-section views. PL at room temperature was carried out with a Perkin Elmer luminescence spectrometer model LS50B, which is controlled by a computer. The samples were excited using a 250 nm (4.96 eV) radiation. PL measurements were scanned between 400 and 900 nm (3.1–1.37 eV) with a resolution of 2.5 nm.

3. Results

The thickness and refractive index of the SRO as deposited films are reported in Table 1. As Ro value changes from 30 to 10, an increasing in the refractive index is observed, indicating the presence of silicon excess in the films. As Ro become higher, the refractive index tends to the SiO_2 value. X-ray photoelectron spectroscopy was used to measure the silicon excess inside of the films. Fig. 1 indicates the composition of the SRO and SI-SRO films with flow ratio, *R*o = 30. For the SRO film, the results indicate a uniform silicon and oxygen profile. The Si and O profile in the SI-SRO film oscillates around the corresponding Si and O profiles of SRO film. These oscillations were a particularity of all the SI-SRO films. This behaviour could be due to the Si implantation because Si and O atoms are displaced from their position. From calculation using SRIM [16] simulation, the expected silicon excess by implantation is around 0.4 at. %. Then, the SI-SRO films should have a 0.4 at. % of silicon excess above of the non-implanted SRO films. However, XPS measurements showed a silicon excess similar to the SRO films, as shown in Fig. 1. The silicon excess varied from 4 to 12.7 at. % depending on the flow ratio (*R*o). A nitrogen profile was also observed, however it is relatively low (around 0.8 at. %) compared to other works reported for SRO PECVD films [11]. Table 2 summarizes the silicon excess in the SRO and SI-SRO films.

Table 2
Silicon excess in SRO and SI-SRO films

Ro=N_2O/SiH_4	Silicon excess (at. %)		
	SRO	Si excess (SRIM) by Implantation	SI-SRO
10	12.7	~0.4	~3.1
20	5.1	~0.4	~5.5
30	4	~0.4	~4.4

Fig. 2 shows the IR absorbance spectra obtained from SRO and SI-SRO films before and after thermal annealing. The presence of some nitrogen characteristic peak is not observed. Only three vibration bands appeared, which are related to Si–O–Si rocking (TO_1), Si–O–Si bending (TO_2) and Si–O–Si stretching (TO_3) [9,15]. For the SRO as deposited film with the highest silicon excess, the TO_1, TO_2 and TO_3 vibration bands were placed at 458, 818 and 1069 cm^{-1}, respectively. The TO_3 band slightly shifted toward higher frequencies and its width reduced as *R*o was increased due to an increment in the oxygen concentration [15]. Another shift and width reduction of the TO_3 vibration band is obtained when the SRO and SI-SRO films were subjected to thermal annealing. The TO_3 vibration band is placed

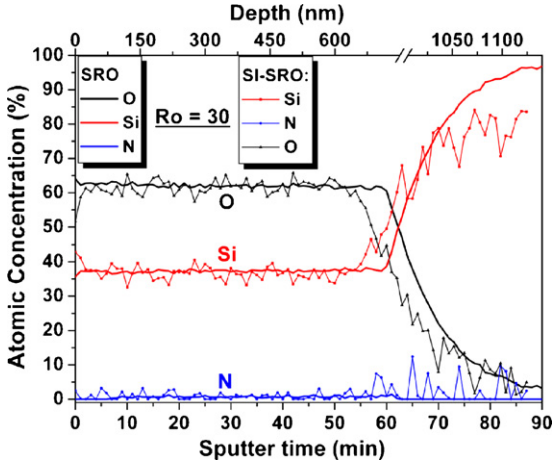

Fig. 1. XPS composition profile of thermally annealed SRO and SI-SRO films with *R*o = 30.

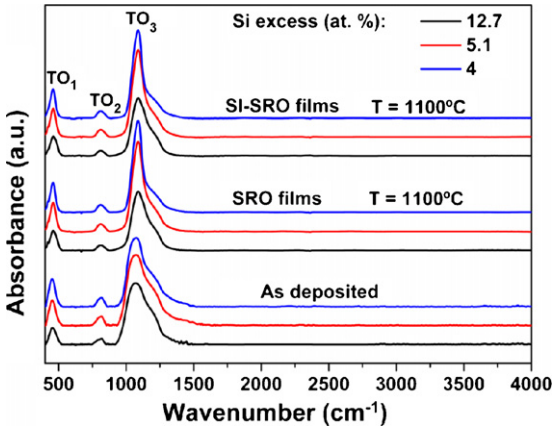

Fig. 2. Infrared absorption spectra of SRO and SI-SRO films before and after thermal annealing.

Table 3
IR vibration bands of SRO and SI-SRO films before and after thermal annealing

Vibration mode	SRO films; Ro=[N_2O/SiH_4]								
	As deposited			Thermally annealed					
				SRO			SI-SRO		
	10	20	30	10	20	30	10	20	30
Si–O Rocking [9,15]	458	452	451	461	461	459	461	461	459
Si–O Bending [9,15]	818	817	817	811	811	811	811	811	811
Si–O Stretching [9,15]	1069	1072	1073	1088	1088	1088	1088	1088	1088

at 1088 cm^{-1} for all films, independently of the flow ratio (*R*o) and silicon implantation. Due to the silicon excess inside these films, we can ascribe these changes to a phase separation of Si and SiO_2. Table 3 summarizes the vibration bands exhibited by the SRO and SI-SRO films before and after thermal annealing.

The structure of the SRO and SI-SRO films was analyzed using an Energy Filtered Transmission Electron Microscopy (EFTEM). Fig. 3 shows the cross view EFTEM images and the size distribution of Si-nanoclusters for the SRO films after thermal annealing. In the images, the bright zones are associated to the presence of silicon in the film.

Fig. 3(a) indicates the presence of silicon agglomeration forming Si-nanoclusters in the SRO film with 12.7 at. % of silicon excess. Some of them are elliptical and some other has an enlarged shape. These last could be due to the agglomeration of nearest Si-clusters. Possibly, most of them could be crystalline. Their size was between 0.5 and 7.5 nm, being the mean size around 4.1 nm as indicated in the histogram.

Fig. 3(b) shows the EFTEM image for the SRO film with 5.1 at. % of silicon excess. Si-nanoclusters are also observed in this film. The image exhibits Si-clusters uniformly distributed into the SRO film. The Si-clusters size extended from 1.5 up to 4 nm, with an average size of 2.7 nm as indicated in the histogram. In this film, the Si-nanoclusters present a spherical shape and agglomeration between Si-clusters is not observed.

On the other hand, Si-clusters were not observed in the SRO film with 4 at. % of silicon excess. Fig. 3(c) exhibits the EFTEM image for this film. Although EFTEM equipment is able to detect Si crystallites or Si clusters of even 1 nm in size, images on several places of the film did not show any silicon agglomeration. However, silicon excess exists within the film, and then Si-clusters could be present inside of this film such as another work has reported [14].

The silicon agglomeration was increased when the SRO film with 5.1 at. % of silicon excess was implanted with silicon (SISRO) and then thermally annealed. Fig. 4 shows the EFTEM image and the histogram of the Si-clusters inside the film. A larger density of clusters is observed. Besides, the number of Si-clusters with size lower than 3 nm was increased if compared to the un-implanted SRO film. The average size of the Si-clusters was around 2.6 nm, almost the same that the SRO film without implantation.

Fig. 5 shows the PL spectra normalized to thickness for the SRO and SI-SRO films thermally annealed. All the films exhibited a PL band in the 1.4–2.1 eV range. A dependence of the PL peak energy and its intensity on the silicon excess is observed. The SRO film with the highest (12.7 at. %) silicon excess emitted a PL peak at 1.62 eV. As the silicon excess was reduced to 5.1 at. %, the PL peak broadness and its intensity increased for 20 times. In spite of a difference in the mean size of the Si clusters between these two films, 4.1 nm for 12.7 at. % and 2.7 nm for 5.1 at. % of silicon excess, the PL peak placed at the same energy. On the other hand, the SRO film with the lowest silicon excess showed a PL peak at a higher energy, 1.69 eV; that is, a redshift took place when the silicon excess was increased from 4 to 5.1 at. %. Although the PL intensity was almost similar, Si-clusters were no observed with the lowest silicon excess. The PL peaks exhibited by the SI-SRO films were at the same energy that SRO films; however, a small increases in the luminescence intensity was obtained with the implantation due to an increasing in the density of Si-clusters.

4. Discussion

The mechanism of light emission observed in silicon based materials has not yet completely understood. So, in SiO_x ($x<2$) films obtained by silicon implantation, the implantation introduces defects such as E centers ($O_3{\equiv}Si^{\bullet}$), neutral oxygen vacancy ($O_3{\equiv}Si{-}Si{-}O_3$), non-bridging oxygen hole centers (NBOHC) ($O_3{\equiv}Si{-}O^{\bullet}$) and D centers [$(Si{\equiv}Si^{\bullet})_n$], besides of interstitial atoms, where some of these defects act as radiative recombination centers. Luminescence in this kind of films is obtained in the blue region of the visible spectra, and it has been related to neutral oxygen vacancies [17]. However, the emission at longer wavelengths has been explained according to two main models: the first one describes that the luminescence take place in silicon nanocrystals by quantum confinement effects (QCE), where the emission is given as a band to band radiative recombination of electron-hole pairs which are confined inside the Si-nc's [7,10, 11]. The second one relates the PL to the presence of defects in the SiO_2/Si-nc matrix and/or interface [12,14].

Si-clusters are created when the SRO films are subjected to high temperature anneal processes due to that the thermal annealing produces a phase separation between Si and SiO_2. Analyzing the obtained FTIR spectra, it can be deduced that a phase separation took place when the SRO and SI-SRO films were thermally annealed due to a displacement of the TO_3 band toward higher frequencies. Although, the EFTEM images only showed silicon agglomeration forming Si-clusters in SRO films with silicon

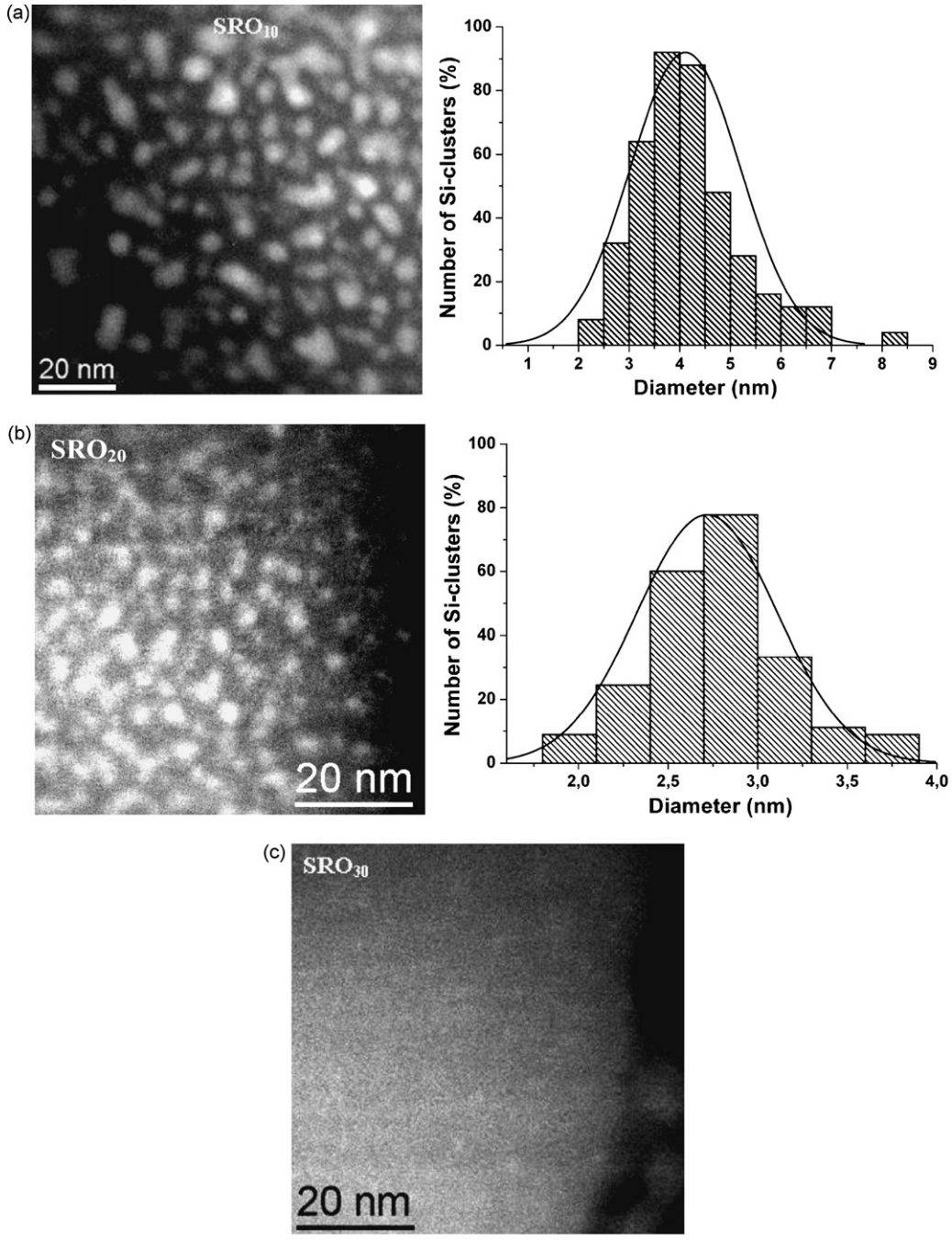

Fig. 3. Cross view EFTEM images and size distribution of Si-clusters in SRO films with (a) 12.7 at. %, (b) 5.1 at. % and (c) 4 at. % of silicon excess annealed at 1100 °C for 60 minutes.

excess higher than 5.1 at. %; it is possible that the low silicon excess in $Ro = 30$ and the thickness of the film does not permit to visualize the silicon agglomeration. Therefore, Si-clusters could be present inside it, however most of them with an average size below 2.7 nm.

In [2], the authors have related the PL of SiO_x ($x < 2$) films to quantum confinement effects (QCE) in materials which contain Si-nc's with a similar size of the Si-clusters obtained in the SRO film with 5 at. % of silicon excess of our experiment. In our experiment, the PL band in 1.62 eV could be correlated to the Si-nanoclusters inside of the SRO film with 5 at. %; however, in the SRO film with the highest silicon excess (12.7 at. %) where the Si-clusters size increased, the PL band strongly reduced and redshift was not observed, contrary to the QCE model. Therefore, other mechanism may be the responsible for the emission in the obtained samples.

As explained before, when the SRO films are thermally annealed, silicon tends to agglomerate, and then Si-nc's, Si-clusters and defects at their surface are created. Therefore, it can be considered that the Si clusters are surrounded by defects and they could be acting as localized states. As a result, the mechanism of emission can be explained as follows: The e-h

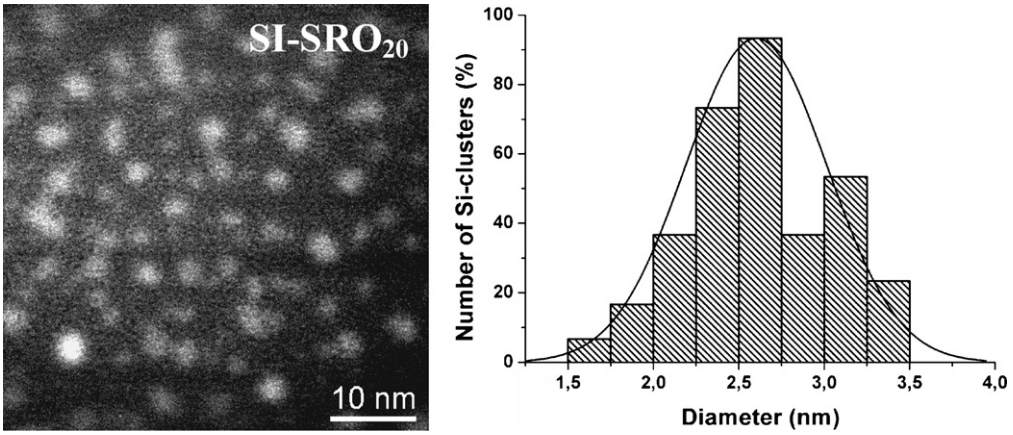

Fig. 4. Cross view EFTEM image and size distribution of Si-clusters for the SI-SRO film with 5.1 at. % of silicon excess annealed at 1100 °C for 60 min.

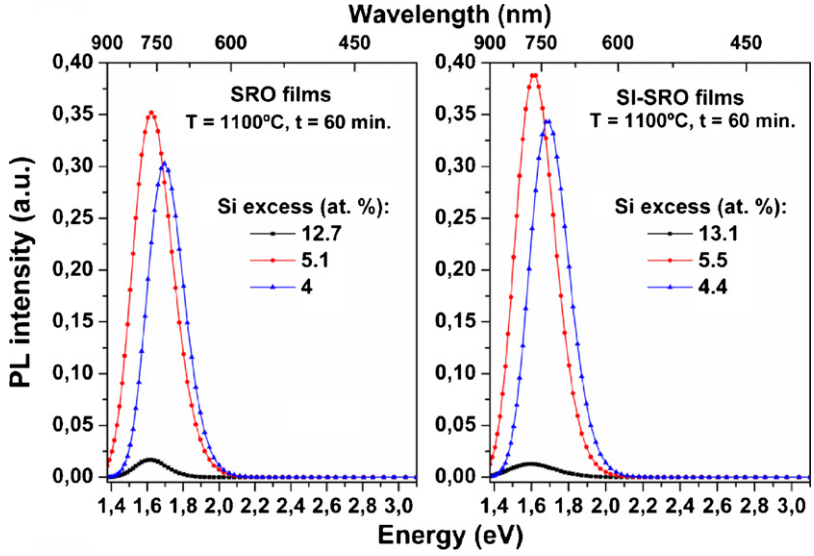

Fig. 5. PL spectra from SRO and SI-SRO films annealed at 1100 °C for 60 min.

pairs are generated inside of the Si-clusters. Then, electrons are excited to the defects, and the emission takes place when electrons in the localized state return to the positive Si-clusters, or the ground state. When the size of the Si- Clusters is small, the band gap energy is large, and then the energy difference between the localized state and the ground state is big enough to produce the emission. This is similar to the donor-acceptor mechanism of emission in semiconductors. As their size increases, this energy difference is reduced, and eventually, when the size exceeds an optimum size, the energy of the localized state will be such that electrons decay will not produce emission, and then PL will not be observed. The optimum size of Si-clusters required in which a maximum PL intensity is observed for our experiments is around 2.7 nm. Because of this, we observe a small redshift when the silicon excess is increased from 4 to 5 at. % and a reduction of the PL intensity when the silicon excess increases to 12.7 at. %.

Fig. 6 shows the dependence of Si-clusters of mean size below 2.7 nm and the PL intensity on the silicon excess in SRO and SI-SRO films emitting at 1.62 eV. For SRO films (SRO_{20} and SRO_{10}), the number of Si-clusters reduces as the silicon excess increases, as a consequence, a strong reduction of the PL intensity in the SRO film with 12.7 at. % of silicon excess was observed. When the SRO_{20} film was implanted with silicon (SI-SRO_{20}), the number of Si-clusters increased producing a more intense photoluminescence.

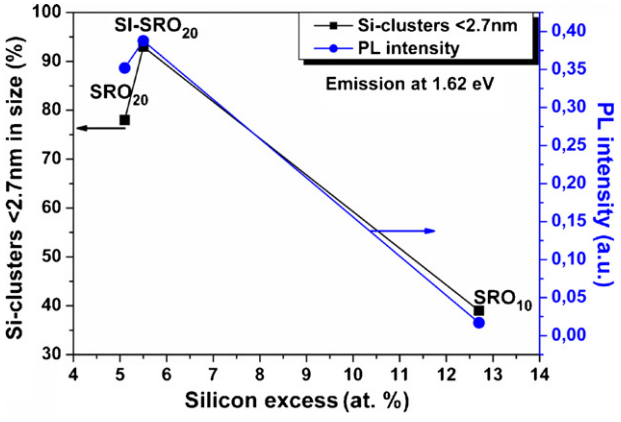

Fig. 6. Dependence of PL intensity and density of Si-clusters with mean size below 2.7 nm on the silicon excess in SRO and SI-SRO films emitting at 1.62 eV.

It is known that the implantation produces a scattering of atoms, then when the SRO films are implanted with silicon (SI-SRO films), Si and O atoms are scattered. Therefore, after the SI-SRO films are subjected to the thermal annealing, a higher density of Si-clusters is obtained to interact with defects and obtain a stronger PL intensity, as observed in the histogram and EFTEM images from Figs. 3(b) and 4. Then, the silicon implantation rather than increasing the size of the Si-cluster, it appears to increase the density of Si-clusters.

5. Conclusions

The composition, structure and optical properties of SRO and SI-SRO films obtained by LPCVD have been studied. The compositional analysis obtained from FTIR did not exhibit vibration bands related to impurities such as H or N neither before nor after thermal annealing. The XPS measurements showed the presence of N in the films; however, its profile was relatively low, around 0.8 at. %. From FTIR spectra, we deduced that a phase separation took place when the SRO films were thermally annealed due to a displacement of the TO_3 band to higher frequencies, and then was corroborated by EFTEM images.

EFTEM analysis showed Si-nanoclusters in the SRO films with silicon excess higher than 5.1 at. %, which were thermally annealed at 1100 °C. The average size of the Si-clusters varied according to the silicon excess, being 2.7 nm for the SRO film with 5.1 at. % and it increased to 4.1 nm for 12.7 at. % of silicon excess. A strong PL was observed in SRO films with 4 and 5.1 at. % of silicon excess. A redshift only took place when the silicon excess was increased between these two films. The photoluminescence strongly reduced when the silicon excess was around 12.7 at. %, where the most of Si-clusters have an average size of 4.1 nm. As a result, the PL origin was related to defects surrounding to the Si-clusters. The silicon implantation increased the density of Si-clusters producing a more intense photoluminescence. The strongest photoluminescence was observed in the SI-SRO film which is annealed at 1100 °C for 60 minutes and having Si-nanoclusters with 2.6 nm in size.

Acknowledgments

Mr A. Morales and Mr J. Barreto acknowledge the grants received from CONACYT and CSIC (I3P), respectively. This work has been partially supported by the project TEC2006-13907/MIC, financed by the Spanish Ministry of Education and Science and P2005MX03 financed by the CSIC/CONACYT.

References

[1] L.T. Canham, Silicon quantum wire array fabrication by electrochemical and chemical dissolution of wafers, Appl. Phys. Lett. 57 (1990) 1046–1048.
[2] E. Kapetanakis, P. Normand, D. Tsoukalas, K. Beltsios, J. Stoemenos, S. Zhang, J. Van den Berg, Charge storage and interface states effects in Si-nanocrystal memory obtained using low-energy Si^+ implantation and annealing, Appl. Phys. Lett. 77 (21) (2000) 3450–3452.
[3] O. Jambois, H. Rinnert, X. Devaux, M. Vergnat, Photoluminescence and electroluminescence of size-controlled silicon nanocrystallites embedded in SiO_2 thin films, J. Appl. Phys. 98 (2005) 046105-1–046105- 3.
[4] Gong-Ru Lin, Chun-Jung Lin, Improved blue-green electroluminescence of metal-oxide-semiconductor diode fabricated on multirecipe Si-implanted and annealed SiO_2/Si substrate, J. Appl. Phys. 95 (12) (2004) 8484–8486.
[5] M. Aceves, J. Carrillo, J. Carranza, W. Calleja, C. Falcony, P. Rosales, Duality metal oxide semiconductor–PN junction in the Al/silicon rich oxide/Si structure as a radiation sensor, Thin Solid Films 373 (2000) 134–136.
[6] K.S. Min, K. Shcheglov, C. Yang, H. Atwater, M. Brongersma, A. Polman, Defect-related versus excitonic visible light emission from ion beam synthesized Si nanocrystals in SiO_2, Appl. Phys. Lett. 69 (14) (1996) 2033–2035.
[7] X.Y. Chen, Y. Lu, Y. Wu, B. Cho, W. Song, D. Dai, Optical properties of SiO_x nanostructured films by pulsed-laser deposition at different substrate temperatures, Appl. Phys. 96 (6) (2004) 3180–3186.
[8] L.B. Ma, A.L. Ji, C. Liu, Y.Q. Wang, Z.X. Cao, Low temperature growth of amorphous Si nanoparticles in oxide matrix for efficient visible photoluminescence, J. Vac. Sci. Technol. B 22 (6) (2004) 2654–2657.
[9] F. Ay, A. Aydinli, Comparative investigation of hydrogen bonding in silicon based PECVD grown dielectrics for optical waveguides, Opt. Mater. 26 (2004) 33–46.
[10] X.Y. Chen, Y. Lu, L. Tang, Y. Wu, B. Cho, X. Xu, J.R. Dong, W.D. Song, Annealing and oxidation of silicon oxide films prepared by plasma-enhanced chemical vapor deposition, J. Appl. Phys. 97 (2005) 014913-1–014913- 10.
[11] F. Iacona, G. Franzó, C. Spinella, Correlation between luminescence and structural properties of Si nanocrystals, J. Appl. Phys. 87 (3) (2000) 1295–1303.
[12] U. Kahler, H. Hofmeister, Silicon nanocrystallites in buried SiO_x layers via direct wafer bonding, Appl. Phys. Lett. 75 (5) (1999) 641–643.
[13] D. Nesheva, C. Raptis, A. Perakis, I. Bineva, Z. Aneva, Z. Levi, S. Alexandrova, H. Hofmeister, J. Appl. Phys. 92 (8) (2002) 4678–4683.
[14] T. Inokuma, Y. Wakayama, T. Muramoto, R. Aoki, Y. Kurata, S. Hasegawa, Optical properties of Silicon clusters and Si nanocrystallites in high-temperature annealed SiO_x films, J. Appl. Phys. 83 (4) (1998) 2228–2234.
[15] P.G. Pai, S.S. Chao, Y. Takagi, Infrared spectroscopic study of SiO_x films produced by plasma enhanced chemical vapor deposition, J. Vac. Sci. Technol. A 4 (3) (1986) 689–694.
[16] J.F. Ziegler, Stopping and Range of Ions in Matter, IBM-Research, New York, 1985.
[17] H.Z. Song, X.M. Bao, N.S. Li, J.Y. Zhang, Relation between electroluminescence and photoluminescence of Si^+-implanted SiO_2, J. Appl. Phys. 82 (8) (1997) 4028–4032.

Biographies

A. Morales Sánchez is a Ph.D. candidate in the Physics department from Autonomous University of Barcelona (UAB), Barcelona, Spain. He received his BS degree in Electronics Engineering from Autonomous University of Puebla (BUAP), Puebla, Mexico, in 2000, and the MS from the National Institute of Astrophysics, Optics and Electronics (INAOE) in Puebla, México, in 2003. Actually, He works on the compositional, structural, optical and electrical properties of materials with silicon nanoparticles for applications in optoelectronic devices.

J. Barreto is a Ph.D. candidate in the Physics department from Autonomous University of Barcelona (UAB), Barcelona, Spain. He received his BS and MS degrees from UAB in 2003 and 2006 respectively. His field of interest is focused on the development of nanostructured-silicon based materials with microelectronic techniques for luminescence applications.

C. Domínguez Horna received the B.S., M.S., and Ph.D. degrees in chemistry from the Universidad Complutense of Madrid, Spain, in 1980, and 1985, respectively. He became a member of the scientific staff at the Instituto de Microelectrónica de Barcelona (IMB-CNM, CSIC) in 1986. Since 1991 he has been a Senior Scientific Researcher. He is involved in materials and process development for new transducers and sensors. Currently he is working on the development of an integrated optical technology based on silicon for (bio)-chemical sensors and broad-band telecommunications applications.

M. Aceves Mijares was born in Mexico City, Mexico. He received the B.S. degree from the Physics and Mathematics School of the National Polytechnic Institute (ESFM-IPN) in Mexico City. The M.S. from the National Institute of Astrophysics, Optics and Electronics (INAOE) in Puebla, Mexico, and the Ph.D. from the Center of Scientific Research of Ensenada (CICESE) in Ensenada, BC, Mexico, both degrees in electrical engineering.He is currently researcher and professor in the electronics department of INAOE. He was research engineer in Gearhart Inc. in Forth worth, Texas, where he worked in the development of high temperature hybrid integrated circuits. He was also a senior engineer in Motorola de Mexico, in Guadalajara, Mexico, where he was involved in the development of quality controls for high power devices. Also, he had been head of different departments in INAOE. He had authored o co-authored over 200 technical papers and had tutored over 50 degree thesis. He was responsible of establishing the microelectronics laboratory of INAOE. He had participated in different technological developments in the microelectronics laboratory of INAOE. His last development was a silicon UV sensor. His research interest is the physic and technology of silicon devices.Dr. Aceves has been awarded with the Esteban de Antuñano price of technology, a commendation from Focus Laser World journal, and a best paper from the Mexican Society of Instrumentation.

J. A. Luna Lopez is a Ph.D. candidate in the Department of electronics of the National Institute of Astrophysics, Optics and Electronics (INAOE) in Puebla, Mexico. He received his BS degree in Electromechanical Engineering from Technologic Institute of Apizaco, Tlaxcala, Mexico, in 1991. MS in the department of Investigation Center Semiconductors Devices (CIDS) from Autonomous University of Puebla (BUAP), Puebla, Mexico, in 2002, He started to work on electrical and optical characterization of the MOS structures. Actually, He works on the structural, optical, electrical and photoelectrical properties of materials with silicon nanoparticles for applications in optoelectronic devices.